Annals of Science and Inquiry
Vol. 2 No. 6 (2026)

Fitted Periodic Components Across Ten Restored Apollo Thermometer Channels

Oliver Collins[1] · Samuel Marshall[2] · Matthew Fisher[3]

[1] Bulgaria · [2] Serbia · [3] Montenegro

Published: June 17, 2026 | Article 849

Abstract

Subsurface temperature channels can yield a numerical phase without supporting a useful paired phase comparison. We fitted a linear background and a fixed 29.53059-day reference component to ten restored Apollo thermometer channels on 79 common observed dates within April–June 1975. The two shallowest retained channels, at 35 and 49 cm, had amplitudes of 2.644690 and 0.880155 K; the other eight ranged from 0.007056 to 0.042755 K. Their paired lower-minus-upper amplitude contrasts included two large negative values and three small positive values whose fixed deletion-window ranges crossed zero. No bridge passed the pre-fixed two-channel phase-reporting rule. These results describe provider-calibrated records and a specified short-window model. They establish neither thermal diffusivity nor a physical phase delay, long-term warming cause or engineering operating condition.

Fitted Periodic Components Across Ten Restored Apollo Thermometer Channels

Abstract

Subsurface temperature channels can yield a numerical phase without supporting a useful paired phase comparison. We fitted a linear background and a fixed 29.53059-day reference component to ten restored Apollo thermometer channels on 79 common observed dates within April-June 1975. The two shallowest retained channels, at 35 and 49 cm, had amplitudes of 2.644690 and 0.880155 K; the other eight ranged from 0.007056 to 0.042755 K. Their paired lower-minus-upper amplitude contrasts included two large negative values and three small positive values whose fixed deletion-window ranges crossed zero. No bridge passed the pre-fixed two-channel phase-reporting rule. These results describe provider-calibrated records and a specified short-window model. They establish neither thermal diffusivity nor a physical phase delay, long-term warming cause or engineering operating condition.

Temperature variation needs a depth and a time basis

An archived temperature is attached to an instrument, a position and an observation time. The restored Apollo heat-flow records retain those distinctions unusually well: the calibrated Apollo 15 and Apollo 17 collections identify individual resistance-temperature detectors, paired bridges and explicit Earth-received times (Nagihara and Nakamura, 2018a) (Nagihara and Nakamura, 2018b). Their temperatures can support a reproducible short-window description even where they cannot support an inferred physical mechanism.

The concatenated archive combines these restored products with older reductions and supplies corrections, quality annotations and convenient representations (St. Clair et al., 2019). Its accompanying research account explains why recovering a time series also requires recovering the meaning of its numbers (St. Clair et al., 2020). We use the original calibrated time and thermometer columns, with a separately verified link to the later quality annotations. This choice avoids silently inheriting a conflicting clock interpretation.

Our question is how a specified periodic component differs across the retained depth channels after a linear background is allowed, and whether the same model justifies displaying a paired phase. The intended quantities are regression coefficients, component amplitude and a conditional phase comparison. They are not the instrument's complete physical uncertainty or lunar heat flux. Defining the measurand before interpreting a number is a basic metrological requirement (JCGM, 2012). Temperatures and temperature amplitudes are expressed in kelvins (BIPM, 2019).

The use of dimensional amplitudes also avoids introducing an arbitrary retention baseline. A fitted oscillation around a background is different from an absolute temperature or a ratio of temperatures. Measurement-scale considerations require retaining the meaning of the transformation (Stevens, 1946). In this study, the temperature depth labels organize the ten observed channels; they are not a manipulated treatment or a fitted universal depth-response curve.

The usable record is smaller than its file inventory

We obtained all six original calibrated gradient-bridge products for day-of-year 092-181 of 1975, a window spanning 2 April through 30 June. The files contain 99,414 bridge records. Each row gives Earth-received time, upper and lower thermometer temperatures, their average, and high- and low-gain temperature differences. Temperature values are rounded to 0.001 K. They were reconstructed by the provider from a shared bridge average and the selected differential measurement, using recovered calibration information. They are not raw independent measurements newly made for this analysis.

The source record contains six bridges, but one cannot support a subsurface comparison. Apollo 15 probe 2's upper bridge has an upper detector about 6 cm above the surface and is documented as frequently saturated. We retain all 17,411 of its rows in the audit while excluding both derived thermometer temperatures from analysis. Its zero quality flags do not override that source warning. The remaining five bridges provide ten channels within four probes at two mission sites.

Their adopted upper/lower depths are 35/84 and 91/139 cm for Apollo 15 probe 1, 49/97 cm for Apollo 15 probe 2, 130/177 cm for Apollo 17 probe 1, and 131/178 cm for Apollo 17 probe 2. The archive documents approximately centimetre-level differences among historical depth descriptions and states which set it adopts. We preserve those adopted labels without treating them as newly surveyed exact positions. Earlier reassessment of Apollo heat-flow interpretation illustrates the care needed when moving from instrument readings to material parameters (Grott et al., 2010).

These are subsurface contact-sensor records. They are also different from orbital surface-temperature products, such as the global Diviner measurements described by Williams and colleagues (Williams et al., 2017). We do not exchange one observation process for the other or infer an unobserved surface boundary from the subsurface channels. The two thermometers in each bridge share reduction inputs, making their errors and reconstructed values dependent. Such shared uncertain inputs matter to interpretation (Carroll et al., 2006).

Retaining the original clock and matching source quality

The primary timestamps are the original explicit day-of-year UTC strings. The later clean-format mission-epoch fields, decoded according to their stated epoch, differ by a constant -22.944 seconds for Apollo 15 and -23.890 seconds for Apollo 17. One clean-product coverage label also retains a conflicting 1971-1974 range. We preserve these discrepancies and do not add or subtract a time offset from the primary records.

For quality matching, we order each representation by its own stored time and pair the ranks within a bridge. Every matched bridge average agrees exactly, and each canonical clean difference equals the negative of an original high- or low-gain difference. This verifies a bijection for source flags without changing the original time field. Three out-of-order records in Apollo 17 probe 2 remain attached to their original row identifiers. Sorting for this audit is different from repairing the measured clock; regression itself does not depend on row order.

We exclude source-marked temperature or difference outliers as entire paired bridge records. The primary analysis window is fixed at 1975-04-02T00:00:00Z through, exclusively, 1975-07-01T00:00:00Z. Its matched date support is the intersection of dates with unflagged observations in every valid bridge: 79 UTC dates. This leaves 75,505 paired records, with both thermometer channels using precisely the same rows within a bridge. Another 6,421 unflagged valid-bridge records fall outside the common dates, and 77 records carry source outlier flags. Every exclusion remains a visible source status.

Matching dates across bridges does not make their sample times identical. We neither interpolate channels into simultaneous measurements nor fill the missing dates. Typical intervals are about 434.71 seconds, while gaps reach roughly five days. The source audit uses an ordinary sample median, including the mean of two central values when appropriate; explicit quantile conventions avoid software ambiguity (Hyndman and Fan, 1996). That median describes cadence and never replaces the actual timestamp differences.

A specified periodic component, not a searched period

Let t be elapsed days from 1975-04-02T00:00:00Z, with 86,400 seconds per analysis day. The fixed reference period P is 29.53059 days, approximately a mean synodic month. It is an analytical reference, not an exact local solar angle, an ephemeris or a recovered forcing time. No frequency is selected by looking for a large fit in these data.

Least-squares frequency analysis can accommodate unequally spaced observations (Lomb, 1976). The statistical interpretation of a spectral search, however, requires additional assumptions about variation and noise (Scargle, 1982). Weighted floating-mean sinusoidal models provide a useful mathematical reference (Zechmeister and Kürster, 2009), but here the frequency is held fixed and a linear background is added. We solve an explicit regression rather than claim a newly detected lunar period.

The channel model is $T(t) = a + b(t-45) + c\cos(2\pi t/P) + s\sin(2\pi t/P) + \text{residual}$. Its four coefficients are estimated separately for each thermometer. Fourier representations distinguish component amplitude and phase from the original time-domain series (Bloomfield, 2000). Ordinary regression reasoning likewise makes coefficients conditional on the chosen predictors (Draper and Smith, 1998). A reference-period fit does not identify the best frequency or prove that its sinusoid represents a particular physical process, a distinction emphasized in periodogram interpretation (VanderPlas, 2018).

Each observed UTC date has equal total weight within its bridge: a record on a date containing n retained samples receives weight 1/n. This specifies representation of dates rather than inverse calibration variance. Weighting choices must state their target (Solon et al., 2015). The result is not a complete 24-hour temperature average. Both channels of a bridge share the same design matrix and weights. Residuals remain serially related time-series observations (Brockwell and Davis, 2016); their large row count does not supply independent sensor replications.

Date balancing also does not repair unequal coverage within a date. A partly observed date can receive the same total weight as a densely observed date, while contributing different observation hours. The fitted basis is evaluated at those actual hours, so it retains their geometry but cannot recover the missing observations. Our deletion exercise changes which observed windows contribute. It cannot establish the temperatures or phases that would have been recorded throughout a gap.

Amplitude is $A = \sqrt{(c^2+s^2)}$, and the residual RMS uses the same date weights. We also report $R = (A/\sqrt{2})/\text{residual RMS}$, a descriptive component-to-residual comparison. It is not a calibrated signal-to-noise ratio or significance statistic. The linear coefficient b absorbs a short-window background; we do not extrapolate it into an annual or multiyear warming rate.

The paired amplitude contrast is specifically A_B-A_A. It is not the amplitude of the temperature-difference series. With a shared design and weights, subtraction of the two fitted coefficient vectors would describe the paired difference channel, but taking a vector magnitude is nonlinear. Subtracting the two magnitudes therefore answers another question. We retain that definition when interpreting a negative contrast: the lower channel's fitted component has a smaller magnitude, without establishing the phase or the magnitude of an oscillating thermal gradient.

A phase number requires more than an inverse tangent

The mathematical peak of the reference component is P atan2(s,c)/(2π), taken modulo P relative to the fixed UTC origin. The paired lag subtracts the upper-channel peak from the lower-channel peak and wraps the result into [-P/2, P/2). Circular representations are necessary for such phase comparisons (Mardia and Jupp, 1999). A positive numerical value would indicate a later fitted peak in the lower channel, not a measured heat-transit time.

The origin specifies a reproducible coordinate for the fitted cycle. It does not identify local sunrise, the thermal maximum at the surface or the instant an RTD equilibrated with surrounding material. Those events would require additional physical and timing information. Preserving an explicit Earth-received time field is useful even for a relative comparison: it makes the temporal representation inspectable without treating an unexplained archival clock difference as an established correction.

Before fitting, we fixed a restrictive display rule. A paired lag appears in the main effect table only if both channels have A greater than 0.001 K and R greater than one in the full fit and in all three fixed deletion fits. The temperature increment and component-over-residual comparison are transparent descriptive screening choices. They are not validated physical reliability limits. Raw mathematical angles remain in the structured outputs even when this rule withholds their display.

This distinction matters because a complete uncertainty assessment would require more than the reported decimal increment. The GUM addresses measurement models and their uncertain inputs (JCGM, 2008). Numerical representation, finite window composition and calibration uncertainty are distinct concerns (Smith, 2013). We do not substitute the fitted residual RMS, the screening rule or a deletion range for an absolute thermometer uncertainty budget.

The three deletions remove [2 April, 2 May), [2 May, 1 June) and [1 June, 1 July), respectively. These are fixed 30-day UTC blocks, not exact lunar cycles. Every refit keeps the original phase origin, trend centering, predictors and date-weighting rule. Their minima and maxima describe finite window sensitivity. Figure 1 shows the connection between calibrated records, matched support and the two empirical comparisons.

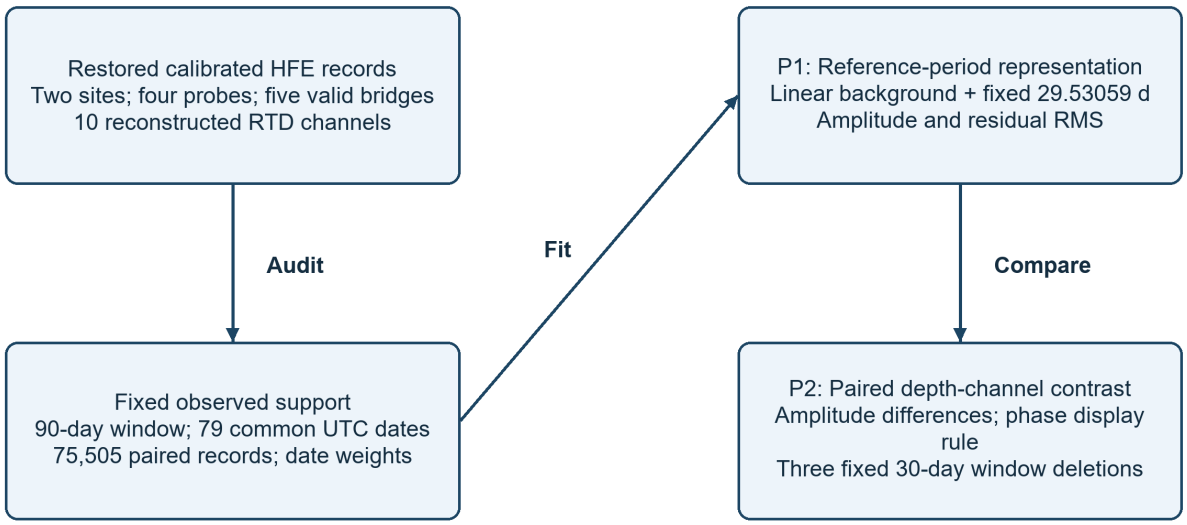

Figure 1. P1 describes the fixed reference-period component after a linear background; P2 compares paired depth channels and applies the pre-fixed phase-display rule. The five bridges share four probes and two sites. Arrows indicate processing, without a causal thermal or engineering model.

Large shallow components coexist with weak deeper fits

The 35 cm channel has a fitted amplitude of 2.644690 K and a residual RMS of 0.488541 K. At 49 cm, the amplitude is 0.880155 K and the residual RMS is 0.130121 K. These two upper channels pass the component display screen in all four fits. The remaining eight amplitudes range from 0.007056 to 0.042755 K, with residual RMS values from 0.023721 to 0.037854 K. Their reference components are small relative to the residual variation under the selected model.

Table 1. Actual full-fit coefficients and amplitudes for all ten channels. Each channel uses 79 observed UTC dates; row counts are serial bridge records rather than independent experimental units. b is a conditional linear-background coefficient. c and s use the fixed UTC phase origin. Numerical parameter digits do not imply calibration accuracy at that precision. Scope is five bridges within four probes and two mission sites.

Channel	Depth (cm)	Records	b (mK/day)	c (mK)	s (mK)	Amplitude (mK)	Residual RMS (mK)	Component/residual RMS
A15P1TG11A	35	15275	-0.482	2215.878	-1443.701	2644.690	488.541	3.828
A15P1TG11B	84	15275	1.242	-6.340	42.282	42.755	37.854	0.799
A15P1TG12A	91	15260	1.150	4.601	-5.350	7.056	23.721	0.210
A15P1TG12B	139	15260	0.445	2.423	-6.966	7.376	23.779	0.219
A15P2TG22A	49	15226	-0.680	866.666	-153.502	880.155	130.121	4.783
A15P2TG22B	97	15226	1.449	12.379	-18.259	22.060	24.606	0.634
A17P1TG11A	130	14882	1.156	-1.070	-8.479	8.546	24.562	0.246
A17P1TG11B	177	14882	0.559	-1.527	-10.129	10.244	29.882	0.242
A17P2TG21A	131	14862	0.478	-2.545	-7.239	7.674	25.871	0.210
A17P2TG21B	178	14862	0.195	-3.350	-6.931	7.699	25.880	0.210

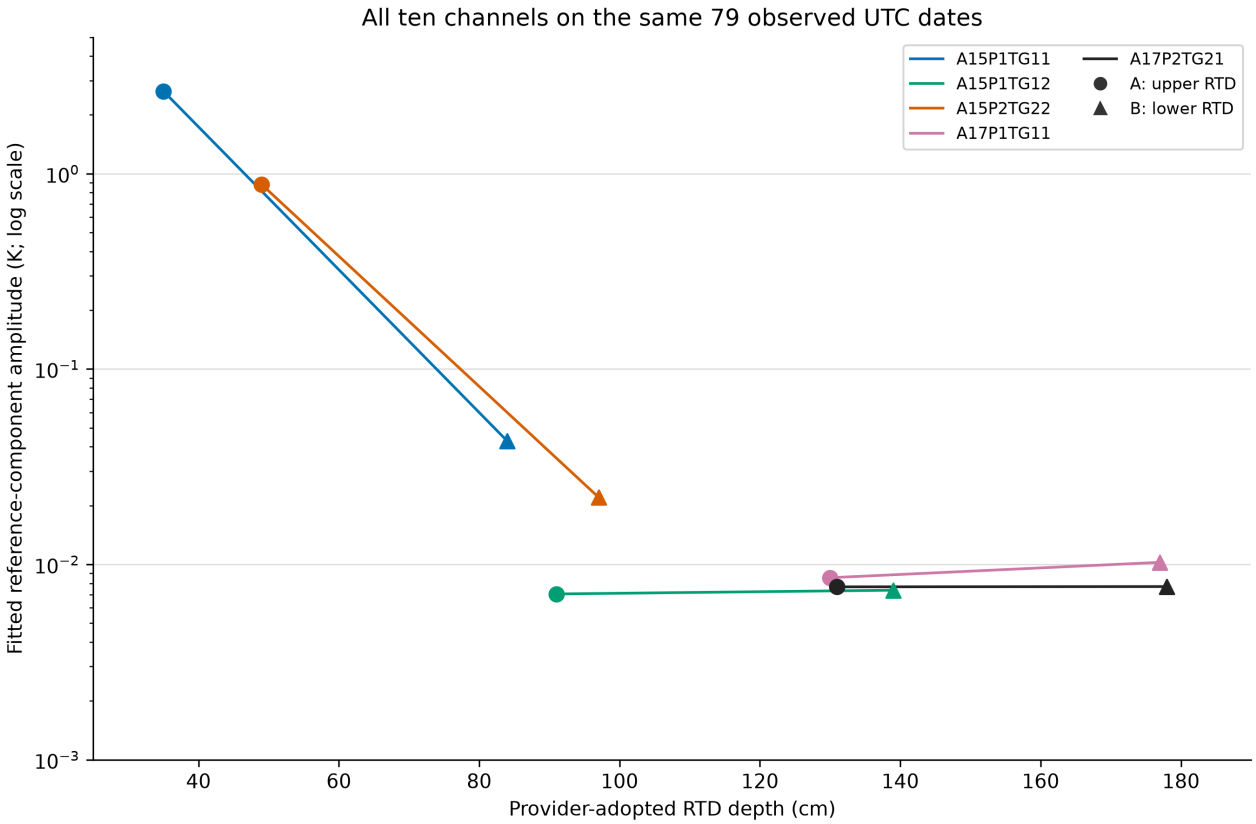

Figure 2. All ten positive full-fit amplitudes on a logarithmic vertical scale. Lines pair upper and lower detectors within each bridge; they do not interpolate a continuous thermal profile. Depths are provider-adopted positions. No population interval or measurement-error bar is shown.

For the 35/84 cm bridge, lower-minus-upper amplitude is -2.601935 K. Its delete-one-window values range from -2.627222 to -2.560474 K. The 49/97 cm bridge gives -0.858095 K, with a range of -0.875930 to -0.848404 K. Both contrasts stay negative in these fixed refits. They are finite differences between represented components, not estimates of a universal depth-decay law.

Table 2. Paired full-fit amplitude effects and finite deletion-window ranges. All three deletion fits retain the same two channels of each bridge and leave out one specified 30-day block. Ranges contain only those three refit values and are not confidence intervals. No bridge meets the phase-display rule, so no paired phase value is reported here.

Bridge	Upper / lower depth (cm)	Paired records	Lower-upper amplitude (K)	Delete-one-window range (K)
A15P1TG11	35 / 84	15275	-2.601935	-2.627222 to -2.560474
A15P1TG12	91 / 139	15260	0.000319	-0.000001 to 0.001021
A15P2TG22	49 / 97	15226	-0.858095	-0.875930 to -0.848404
A17P1TG11	130 / 177	14882	0.001698	-0.000138 to 0.002765
A17P2TG21	131 / 178	14862	0.000025	-0.000119 to 0.000024

The other three full-fit contrasts are positive but small: approximately 0.319, 1.698 and 0.025 mK. Each corresponding deletion range includes both signs. These values do not establish an ordered physical amplitude profile at the deeper positions. Some numerical contrasts are smaller than one published temperature increment; averaging many correlated reconstructed values does not itself establish sub-increment calibration accuracy.

No bridge has two channels that pass the phase-display rule across the full fit and every deletion. We therefore report no paired phase estimate in the main results. This outcome concerns the stated model and reporting decision. It does not prove that the subsurface lacks periodic forcing, and it does not mean that the mathematical inverse tangent could not be calculated. The raw coefficients and angles permit that distinction to be inspected.

Processing sensitivity is part of the same comparison

The fixed quality sensitivity adds marked records within the same 79 dates while continuing to exclude the source-invalid bridge. It adds 74 records in total; three other marked records occur outside the common dates. Table 3 includes every valid bridge. The large 35/84 cm contrast changes by -0.022027 K. Two small positive contrasts become negative when marked points are included. No filter is selected on the basis of those changes.

Table 3. Source-outlier inclusion diagnostic using the same dates, reference model and weighting rule. Changes are deterministic processing differences. Saturated above-surface-bridge records remain excluded from both versions. This diagnostic neither corrects the original calibration nor supplies a population uncertainty interval.

Bridge	Added marked records	Primary contrast (K)	Include-marked contrast (K)	Change (K)
A15P1TG11	10	-2.601935	-2.623963	-0.022027
A15P1TG12	6	0.000319	-0.000115	-0.000434
A15P2TG22	13	-0.858095	-0.854580	0.003515
A17P1TG11	26	0.001698	0.001288	-0.000409
A17P2TG21	19	0.000025	-0.000063	-0.000088

The lunar context does not turn these regressions into an operating-temperature model. Lunar-Bench's Table 10 gives a thermal scraper's 50°C activation setpoint as part of a sampling scenario (Xiao et al., 2026). A device setpoint and a regolith background temperature with a stated depth and time are different inputs. The Apollo records do not validate that setpoint, the scenario's tool choice, its model scores or conditions in the South Pole-Aitken Basin.

Physical conduction models require geometry, properties and boundary conditions beyond a sinusoidal description (Carslaw and Jaeger, 1959). Recovering an unknown heating action from subsurface temperatures is an inverse problem with additional assumptions (Woodbury et al., 2023). We perform neither inversion. Installation effects, possible heater operations, calibration structure and unmodeled thermal changes remain relevant without being separately identified here. The short-window linear backgrounds cannot identify the cause of long-term warming.

A finite and reproducible temperature description

The observational scope is ten dependent channels, four probes and two sites. It is not a random sample of lunar subsurface environments, and sampling-based generalization would require a design absent from these records (Neyman, 1934). With roughly three reference periods in the entire window, deleting one block also leaves a short description rather than an independent replication. We give coefficients and finite ranges without confidence coverage or statistical significance claims.

The primary computation uses weighted linear least squares. An independent calculation rereads every original ASCII value and quality match, forms scalar weighted moments and solves the four-parameter equations in 55-digit decimal arithmetic. Numerical linear algebra distinguishes such implementation

checks from assumptions about the data-generating process (Golub and Van Loan, 2013). All 80 channel fits, including both quality versions and all deletions, reproduce. Coefficient differences are below 6.3×10^{-12} in their corresponding units, and full-prediction differences are below 6.5×10^{-12} K.

The source audit retains original row identifiers, clocks, detector labels, calibration-derived fields and excluded states. Fitness for reuse depends on these meanings as well as on numerical correctness (Wang and Strong, 1996). Original files, checksums, the frozen secondary-analysis protocol and all fitted outputs remain linked for computational reproduction (Peng, 2011). Their provenance and declared limitations support FAIR reuse (Wilkinson et al., 2016). No new lunar experiment, language-model evaluation or operating recommendation was undertaken. Accountable human source verification and final approval remain pending.

References

1. Zechmeister, M.; Kürster, M.. (2009). The generalised Lomb-Scargle periodogram: A new formalism for the floating-mean and Keplerian periodograms. Astronomy & Astrophysics. https://doi.org/10.1051/0004-6361:200811296
2. VanderPlas, Jacob T.. (2018). Understanding the Lomb-Scargle Periodogram. The Astrophysical Journal Supplement Series. https://doi.org/10.3847/1538-4365/aab766
3. Grott, M.; Knollenberg, J.; Krause, C.. (2010). Apollo lunar heat flow experiment revisited: A critical reassessment of the in situ thermal conductivity determination. Journal of Geophysical Research: Planets. https://doi.org/10.1029/2010je003612
4. Xiao, Xin-Yu; Tian, Ye; Yin, Erwei; He, Zhixian; Wang, Shiqi; Liu, Yalei; Xia, Qianchen. (2026). Lunar-Bench: Towards Evaluating Task-Oriented Reasoning of LLMs in Lunar Exploration Scenarios. Findings of the Association for Computational Linguistics: ACL 2026. https://aclanthology.org/2026.findings-acl.83/.
5. Bureau International des Poids et Mesures. (2019). The International System of Units (SI),9th edition,version3.01(August2024). https://www.bipm.org/documents/20126/41483022/SI-Brochure-9-EN.pdf/2d2b50bf-f2b4-9661-f402-5f9d66e4b507?version=4.0
6. Mardia, Kanti V.; Jupp, Peter E.. (1999). Directional Statistics. Wiley Series in Probability and Statistics. https://doi.org/10.1002/9780470316979
7. Brockwell, Peter J.; Davis, Richard A.. (2016). Introduction to Time Series and Forecasting. Springer Texts in Statistics. https://doi.org/10.1007/978-3-319-29854-2
8. Woodbury, Keith A.; Najafi, Hamidreza; de Monte, Filippo; Beck, James V. (2023). Inverse Heat Conduction Problems: An Overview. In Inverse Heat Conduction,pp.1-23. Wiley. https://doi.org/10.1002/9781119840220.ch1
9. Wilkinson, Mark D.; Dumontier, Michel; Aalbersberg, IJsbrand Jan; Appleton, Gabrielle; Axton, Myles; Baak, Arie; Blomberg, Niklas; Boiten, Jan-Willem; da Silva Santos, Luiz Bonino; Bourne, Philip E.; Bouwman, Jildau; Brookes, Anthony J.; Clark, Tim; Crosas, Mercè; Dillo, Ingrid; Dumon, Olivier; Edmunds, Scott; Evelo, Chris T.; Finkers, Richard; Gonzalez-Beltran, Alejandra; Gray, Alasdair J.G.; Groth, Paul; Goble, Carole; Grethe, Jeffrey S.; Heringa, Jaap; 't Hoen, Peter A.C; Hooft, Rob; Kuhn, Tobias; Kok, Ruben; Kok, Joost; Lusher, Scott J.; Martone, Maryann E.; Mons, Albert; Packer, Abel L.; Persson, Bengt; Rocca-Serra, Philippe; Roos, Marco; van Schaik, Rene; Sansone, Susanna-Assunta; Schultes, Erik; Sengstag, Thierry; Slater, Ted; Strawn, George; Swertz, Morris A.; Thompson, Mark; van der Lei, Johan; van Mulligen, Erik; Velterop, Jan; Waagmeester, Andra; Wittenburg, Peter; Wolstencroft, Katherine; Zhao, Jun; Mons, Barend. (2016). The FAIR Guiding Principles for scientific data management and stewardship. Scientific Data. https://doi.org/10.1038/sdata.2016.18.
10. Stevens, S. S.. (1946). On the Theory of Scales of Measurement. Science. https://doi.org/10.1126/science.103.2684.677.
11. Scargle, J. D.. (1982). Studies in astronomical time series analysis. II - Statistical aspects of spectral analysis of unevenly spaced data. The Astrophysical Journal. https://doi.org/10.1086/160554
12. St. Clair, Michael; Million, Chase; Siegler, Matthew. (2019). Apollo 15 and17 Heat Flow Experiment Concatenated Data Sets Bundle,version1.0; data collectionversion2.0. Edited by Jennifer Ward. NASA Planetary Data System. https://doi.org/10.17189/1518441
13. Joint Committee for Guides in Metrology. (2012). International vocabulary of metrology - Basic and general concepts and associated terms (VIM), third edition (JCGM200:2012). Bureau International des Poids et Mesures. https://doi.org/10.59161/JCGM200-2012

14. Hyndman, Rob J.; Fan, Yanan. (1996). Sample Quantiles in Statistical Packages. The American Statistician. https://doi.org/10.1080/00031305.1996.10473566

15. Golub, Gene H.; Van Loan, Charles F. (2013). Matrix Computations,4th edition. Johns Hopkins University Press. https://doi.org/10.56021/9781421407944

16. Joint Committee for Guides in Metrology. (2008). Evaluation of measurement data - Guide to the expression of uncertainty in measurement (JCGM100:2008). Bureau International des Poids et Mesures. https://doi.org/10.59161/JCGM100-2008E

17. Bloomfield, Peter. (2000). Fourier Analysis of Time Series: An Introduction. Wiley Series in Probability and Statistics. https://doi.org/10.1002/0471722235

18. Carroll, Raymond J., David Ruppert, Leonard A. Stefanski, and Ciprian M. Crainiceanu. “Measurement Error in Nonlinear Models.” 2006. https://doi.org/10.1201/9781420010138.

19. Nagihara, Seiichi; Nakamura, Yosio. (2018). Apollo 17 ALSEP ARCSAV Heat Flow Experiment Calibrated Gradient Bridge Temperatures Bundle,version1.0. NASA Planetary Data System. Edited by D.R.Williams and S.A.McLaughlin. https://doi.org/10.17189/1518451

20. Williams, J.-P.; Paige, D.A.; Greenhagen, B.T.; Sefton-Nash, E.. (2017). The global surface temperatures of the Moon as measured by the Diviner Lunar Radiometer Experiment. Icarus. https://doi.org/10.1016/j.icarus.2016.08.012

21. Smith, Ralph C.. (2013). Uncertainty Quantification: Theory, Implementation, and Applications. Society for Industrial and Applied Mathematics. https://doi.org/10.1137/1.9781611973228

22. St. Clair, Michael; Million, Chase; Siegler, Matthew. (2020). Improvements to the Apollo 15 and 17 heat flow experiment data archive. Planetary and Space Science. https://doi.org/10.1016/j.pss.2020.104944

23. Draper, Norman R.; Smith, Harry. (1998). Applied Regression Analysis. Wiley Series in Probability and Statistics. https://doi.org/10.1002/9781118625590

24. Solon, Gary; Haider, Steven J.; Wooldridge, Jeffrey M.. (2015). What Are We Weighting For?. Journal of Human Resources. https://doi.org/10.3368/jhr.50.2.301.

25. Lomb, N. R.. (1976). Least-squares frequency analysis of unequally spaced data. Astrophysics and Space Science. https://doi.org/10.1007/bf00648343

26. Nagihara, Seiichi; Nakamura, Yosio. (2018). Apollo 15 ALSEP ARCSAV Heat Flow Experiment Calibrated Gradient Bridge Temperatures Bundle,version1.0. NASA Planetary Data System. Edited by D.R.Williams and S.A.McLaughlin. https://doi.org/10.17189/1518442

27. Wang, Richard Y.; Strong, Diane M.. (1996). Beyond Accuracy: What Data Quality Means to Data Consumers. Journal of Management Information Systems. https://doi.org/10.1080/07421222.1996.11518099

28. Neyman, Jerzy. (1934). On the Two Different Aspects of the Representative Method: The Method of Stratified Sampling and the Method of Purposive Selection. Journal of the Royal Statistical Society,97(4),558-606. https://doi.org/10.1111/j.2397-2335.1934.tb04184.x.

29. Peng, Roger D.. (2011). Reproducible Research in Computational Science. Science. https://doi.org/10.1126/science.1213847

30. Carslaw, Horatio Scott; Jaeger, John Conrad. (1959). Conduction of Heat in Solids,2nd edition. Clarendon Press. https://books.google.com/books?id=y20sAAAAYAAJ